100 Gb/s Optical Time-Division Multiplexed Networks

Scott A. Hamilton, *Member, IEEE,* Bryan S. Robinson, *Student Member, IEEE,* Thomas E. Murphy, *Member, IEEE,* Shelby Jay Savage, *Member, IEEE,* and Erich P. Ippen, *Fellow, IEEE*

Invited Paper

***Abstract*—We present ultrafast slotted optical time-division multiplexed networks as a viable means of implementing a highly capable next-generation all-optical packet-switched network. Such a network is capable of providing simple network management, the ability to support variable quality-of-service, self-routing of packets, scalability in the number of users, and the use of digital regeneration, buffering, and encryption. We review all-optical switch and Boolean logic gate implementations using an ultrafast nonlinear interferometers (UNIs) that arecapable of stable, pattern-independent operation at speeds in excess of 100 Gb/s. We expand the capability provided by the UNI beyond switching and logic demonstrations to include system-level functions such as packet synchronization, address comparison, and rate conversion. We use these advanced all-optical signal processing capabilities to demonstrate a slotted OTDM multiaccess network testbed operating at 112.5 Gb/s line rates with inherent scalability in the number of users and system line rates. We also report on long-haul propagation of short optical pulses in fiber and all-optical 3R regeneration as a viable cost-effective means of extending the long-haul distance of our OTDM network to distances much greater than 100 km.**

***Index Terms*—3R regeneration, address comparison, demultiplexing, folded ultrafast nonlinear interferometer, intersymbol interference, laser amplifiers, long-haul transmission, optical communication, optical logic devices, optical logic gates, optical packet switching, optical processing, optical propagation, optical switching, optical time-division multiplexing, polarization stabilization, pulse-position modulation, pulse time modulation, rate conversion, synchronization, time division multi-access, time division multiplexing, ultrafast networks, ultrafast nonlinear interferometer.**

I. Introduction

THE growth of the Internet has led to a surge in demand for bandwidth in telecommunications networks. This trend, along with the changing nature of the traffic from voice to primarily data traffic, has stimulated the rapid evolution of optical networking technologies in recent years. In the first-generation terrestrial optical networks deployed today, high-speed electronic routers are interconnected by optical fiber links utilizing wavelength division multiplexing (WDM). In order to achieve packet routing, the optical signal entering the router is converted to an electronic signal and demultiplexed into lower-rate streams that are electronically routed in the switch core and then remultiplexed to a high-speed electronic signal that is output from the router on the specified optical wavelength. This optical-electronic-optical conversion leads to router congestion and reduced throughput in today's networks. Because transmission rates continue to increase in optical fiber much faster than electronic processing speeds, work is underway to develop second-generation optical networks that provide continuous optical paths using optical cross-connects (OXCs) and optical add-drop multiplexers (OADMs). With these technologies, individual wavelength channels can be routed between nodes or switched on/off the network using all-optical techniques. In order to achieve truly flexible packet switching with granularity that extends beyond single wavelength channels to individual packets, third-generation optical packet-switched networks with optical routers connected to the OXCs and OADMs in the optical transport layer are envisioned. The addition of optical routers in third-generation packet-switched networks will allow active packet routing within and between wavelengths while simultaneously providing an optical path that is transparent to both data format and transmission rate. Third-generation packet-switched networks are expected to provide many advantages compared to earlier architectures. First, low-level network functionality such as routing is distributed in the optical network core, while high-level processing such as network management and user access scheduling is pushed to the network edges. Because payload data is transparent in a packet-switched network, each switch can remain in any given state for an arbitrary amount of time, and a wide range of services from best-effort datagram, to virtual-circuit connections, to guaranteed bandwidth via a dedicated lightpath can be provided simultaneously. Third-generation optical packet-switched networks may also provide scalability and flexibility to efficiently handle time-dependent network traffic patterns.

In today's first-generation networks, optical technology has been inserted only at the physical layer of the multilayer pro-

Manuscript received June 3, 2002; revised September 30, 2002. This work was sponsored by the Defense Advanced Research Projects Agency under Air Force Contract F19628-00-C-0002.

S. A. Hamilton, B. S. Robinson, and S. J. Savage are with the Optical Communications Technology Group, Lincoln Laboratory, Massachusetts Institute of Technology, Lexington, MA 02420 USA (e-mail: shamilton@ll.mit.edu).

T. E. Murphy was with Lincoln Laboratory, Massachusetts Institute of Technology, Lexington, MA 02420 USA. He is now with Department of Electrical and Computer Engineering, University of Maryland, College Park, MD 20742 USA.

E. P. Ippen is with the Research Laboratory of Electronics, Department of Electrical Engineering and Computer Science, Massachusetts Institute of Technology, Cambridge, MA 02139 USA.

Digital Object Identifier 10.1109/JLT.2002.806781

0733-8724/02$17.00 © 2002 IEEE

tocol stack. For practical reasons, this first step makes sense because it allows straightforward extension of existing networks into the optical regime, without any modification of the higher layers. While the use of optical technology in today's first-generation networks has been utilized to increase existing network capacity, such an architecture does not fully utilize the advantages offered by optical networking.

Second-generation optical networks that achieve routing and switching with wavelength granularity are possible today due to the development of new optical components such as integrated tunable lasers, wideband spectrally flattened optical amplifiers, fiber Bragg grating wavelength routers, and cross-connect switches. In such a WDM network, electronic rate data is modulated onto multiple wavelength channels that can propagate through an optical fiber with minimal interchannel interference. At present, WDM networks with individual wavelength channel rates of 10 Gb/s are being deployed, with 40 Gb/s equipment under development. Due to the large number of wavelength channels that must be processed at each node and the lack of practical optical buffers, resource management and control in a WDM network can be challenging. These functions are generally achieved using a central network resource scheduler that coordinates network access and source/destination wavelength allocation.

In optical time-division multiplexed (OTDM) networks, the fiber bandwidth is available in a single (or few) high bit-rate wavelength channel(s) instead of being distributed across many distinct WDM channels. In bit-interleaved OTDM networks (e.g., [1], [2]), electronic data from an individual user is modulated onto a short-pulse train with a repetition rate that matches the original electronic data rate (i.e., 10 Gb/s). To achieve high spectral efficiency in a bit-interleaved OTDM network, short optical pulse trains from multiple users can be bit-interleaved in time with minimal interchannel interference. Bit-interleaved OTDM and WDM systems are similar because the fiber bandwidth is divided into a large number of lower-rate channels. Also, centralized management of resources is required and current switching technologies preclude any user from accessing the entire bandwidth of the network at any given time. Therefore, from an architectural point-of-view, bit-interleaved OTDM systems are identical to WDM systems.

Slotted OTDM networks [3]–[7] are fundamentally different from bit-interleaved OTDM and WDM systems. Time is partitioned into slots containing tens-of-thousands of bits and each access node is capable of bursting data into these slots at the ultrafast channel rate ($>$100 Gbs). Because the data is packetized, slotted OTDM systems can provide better network performance in terms of throughput and delays through statistical multiplexing of multiple user traffic. Also, centralized network management is simpler because the signaling information needed for resource allocation is contained in the slot header. Slotted OTDM networks have the potential to provide all-optical packet-switching functionality. For both high-end users capable of transmission bursts at very high rates and large sets of low-rate users, all-optical packet switching in slotted OTDM networks will enable both guaranteed bandwidth and bandwidth-on-demand network services. Another advantage for OTDM systems is that single-channel ultrafast optical pulse streams can be all-optically regenerated in order to expand network transmission distances.

In this paper, we discuss our efforts to implement ultrafast devices, packet processing functionality for OTDM networks, long-haul short-pulse propagation, and all-optical 3R regeneration. Each of these topical areas are required in order to implement packet switching for third-generation all-optical networks. Beginning with key components for slotted OTDM systems, we discuss the ultrafast nonlinear interferometer optical logic gate and the use of pulse-position modulation to achieve data pattern-independent functionality. We also present current results in which we demonstrate OTDM testbed operation at single channel line rates of 112.5 Gb/s. Network-wide self-synchronization is achieved using global clock distribution and a single optical logic gate. We achieve all-optical 4-bit address comparison and transmit and receive OTDM slots fully loaded with 100 Gb/s pseudorandom binary sequence data. Finally, we describe our work in long-haul propagation of short optical pulses and all-optical regeneration using the folded ultrafast nonlinear interferometer.

II. Ultrafast Optical Logic

All-optical switches and logic gates are capable of high-speed operation ($>$ 100 Gb/s per channel) and low power consumption (typical switching energies $<$ 20 fJ per pulse). A key parameter that influences the design of an all-optical component is the nonlinear material. Past demonstrations of all-optical components were implemented using discrete optical devices and exploited third-order nonlinear processes in active semiconductor material or optical fiber. Various optical switch and logic gate architectures have been developed to date. Examples of semiconductor-based optical switches implemented with discrete components include demultiplexers [8]–[13], wavelength converters [14], [15], pass gates [16], add-drop multiplexers [17], and optical regenerators [18], [19]. Demonstrations of optical fiber switches include demultiplexers [20]–[22], pass gates [23], and optical regenerators [24], [25]. Optical logic gates have also been developed using semiconductor material and discrete components for Boolean operations including AND [26], [27], OR [26], and XOR [28] gates. Demonstrations of optical fiber logic gates include AND [29] and XOR [20], [30] gates.

Optical switches will ultimately be feasible in larger systems only if they can be significantly reduced in size and monolithically integrated with high yield. These requirements are difficult to satisfy using optical fiber switches. However, the nonlinear response of semiconductor material is typically four orders of magnitude larger than in fiber and the required interaction length is typically less than 1 mm. This comparatively small interaction length and potential for multiswitch integration has resulted in the development of a Mach–Zehnder switch structure in which a semiconductor optical amplifier (SOA) is placed in each arm of the interferometer [31]. These single switches and logic gates are typically a few millimeters in length and have been demonstrated for a variety of applications including demultiplexing [32]–[36], wavelength conversion [32], [37], add-drop multiplexing [34], optical regeneration [32], OR gates [38], and XOR [39] gates.

Although the large nonlinear response of semiconductor material is attractive, semiconductor-based optical switches are

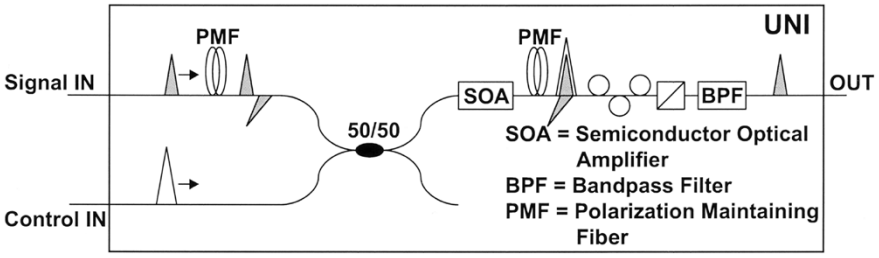

Fig. 1. Ultrafast nonlinear interferometer all-optical switch and logic gate.

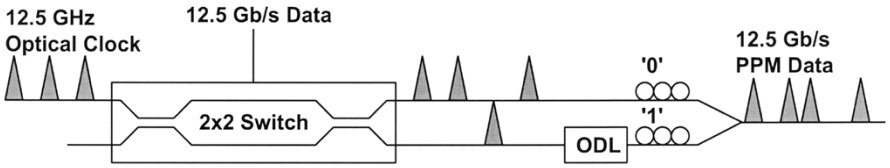

Fig. 2. Pulse position modulator.

challenging to implement in practice due to the different physical components and response times that contribute to the total material nonlinearity. Pump-probe experiments have been used to characterize the various nonlinear mechanisms in InGaAsP waveguides [40]. In addition to subpicosecond components of the semiconductor nonlinearity resulting from two-photon absorption, spectral-hole burning and carrier heating, interband carrier dynamics lead to long-lived refractive index and gain nonlinearities which have a recovery time between 100 to 1000 picoseconds. The carrier lifetime may be reduced to a few tens of picoseconds by operating at high carrier densities or by the use of optical holding beams [41], [42]. Even after reducing the carrier lifetime, interband dynamics can limit the maximum operational speed of an all-optical switch.

The ultrafast nonlinear interferometer (UNI) [12], [26], [27] is a switch geometry that eliminates the operational speed limits imposed by data pattern-dependent long-lived refractive index nonlinearities in semiconductor material. A block diagram of the UNI is shown in Fig. 1. The signal pulse input to the switch is split in birefringent fiber into two orthogonally polarized temporally-separated components. The control pulse input is combined via a 50/50 coupler and set to temporally overlap one of the orthogonal signal pulse components at the SOA nonlinear medium. Via cross-phase modulation (XPM), the control pulse imparts a nonlinear phase shift on the overlapped signal pulse component. After propagation through a second piece of cross-spliced birefringent fiber, the two signal pulse components are reset to temporally overlap and then interfere together at a polarizer set at 45° with respect to the orthogonal signal polarizations. At the output of the switch, the control pulse is removed by a bandpass filter tuned to the signal wavelength.

Because the UNI is a single-arm interferometer, the switch is stable with respect to length changes because both signal components travel along an identical path through the device. The UNI also eliminates data pattern-dependent long-lived refractive index changes because both signal components pass through the nonlinear medium. The interferometer is balanced because both signal components experience phase changes that occur over time scales longer than their temporal separation, whereas only the signal pulse component overlapped by the control pulse experiences the additional nonlinear phase shift due to the ultrafast components in the semiconductor nonlinear response. Because the long-lived index of refraction changes are cancelled, the UNI provides a balanced interferometric output.

In addition to the UNI, various balanced interferometer designs [8], [10], [16], [17], [31] have been used to compensate for the long-lived index changes in the semiconductor. However, gain-saturation remains a problem and leads to pattern-dependent amplitude modulation at the output of the switch, especially when data is injected into the control port of the UNI. Several methods for reducing the effects of gain-saturation in SOAs used for in-line amplification of nonreturn-to-zero (NRZ) systems have been recently proposed [43], [44]. These techniques maintain a constant intensity in the SOA by modulating both the data and the inverse data on orthogonal polarizations or wavelengths. They are not easily extended to return-to-zero (RZ) formats such as those used in optical time-division multiplexed networks.

By contrast, pulse-position modulation (PPM) is a modulation format with a constant energy-per-bit that can be easily implemented in existing OTDM architectures. With PPM, a pulse exists in every bit slot, ensuring a constant energy-per-bit. Information is conveyed via the temporal placement of the pulse within the bit slot. In the present paper, we use a binary PPM format where a pulse in the first half of the bit slot represents a "0," while a pulse in the second half of the bit slot represents a "1." Thus, at a data rate of 112.5 Gb/s (8.8 ps/bit), the difference in arrival time between a "1" and a "0" is only 4.4 ps. Since this temporal separation is much shorter than the gain recovery time of the SOA, patterning due to gain-saturation is greatly reduced as compared to other intensity modulation formats [45].

To generate a pseudorandom stream of binary PPM pulses, we use the setup shown in Fig. 2. A mode-locked fiber laser emitting pulses at a repetition rate of 12.5 GHz is used as the input to a 2×2 $LiNbO_3$ modulator. A 12.5 Gb/s NRZ pseudorandom binary sequence from a pulse-pattern generator causes

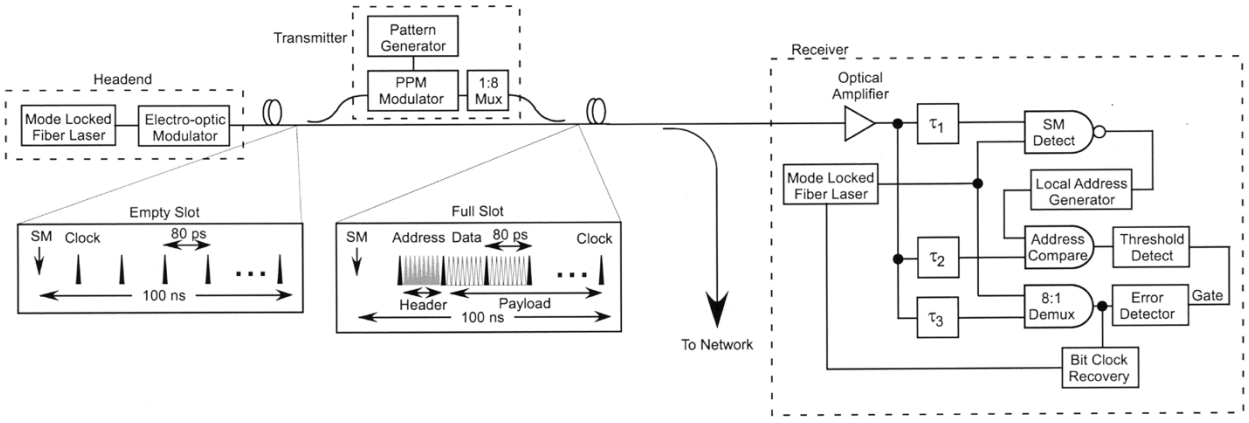

Fig. 3. Synchronous OTDM testbed headend, transmitter, and receiver configuration and network slot architecture.

the modulator to switch between cross and bar states. This produces an RZ on-off-keyed (OOK) version of the data in one output arm of the switch and the inverse of the data in the other output of the switch. A variable optical delay line (ODL) in one of the arms introduces the temporal PPM offset. The two pulse streams are then recombined in a 50/50 polarization maintaining coupler to produce the PPM data stream. Because of its inherently stable operation and ultrafast response, we use the UNI with PPM data formatting to provide multiple all-optical logic and switching functions such as packet synchronization, address comparison, and demultiplexing at rates in excess of 100 Gb/s in our OTDM system testbed demonstration.

III. OTDM System Description

At present, the majority of research on ultrafast optical networks has been focused on device technology demonstrations such as all-optical logic at OTDM rates [27], high repetition-rate short pulse optical sources [46], self-synchronization techniques [47], wavelength conversion [14], and short pulse long-haul propagation [48]. Although the number of OTDM systems in which end-to-end packet processing at the line rate is demonstrated has been limited, significant progress has been made in various areas including single-bit [49] and multiple-bit [50], [51] all-optical address comparison and packet routing at OTDM rates and receiver slot self-synchronization [50], [51]. Recent demonstrations of systems that provide both packet synchronization and address processing are described in [49]–[54]. In [51], two passively mode-locked lasers are bit-phase-synchronized via an active control circuit. System synchronization to incoming network packet timing is achieved, however, by manually setting an optical delay line. In [49], [50], a single clock pulse orthogonally polarized to the address bits was used for system synchronization to packet timing and local receiver address generation [50]. An alternative means of system synchronization to incoming packet timing, which requires correlation detection of two marker pulses with an offset spacing of 1.5-bit periods, is also described in [50].

Each of these packet-level system synchronization techniques [49]–[51] presents a system designer with significant challenges when the transmitter and receiver are separated by long optical fiber spans. Manual delay lines require active monitoring due to environmentally induced delay variations. Orthogonally polarized clock and address pulses are difficult to maintain due to polarization-mode dispersion inherent in optical fiber spans and prevent increased spectral efficiency through polarization multiplexing [55]. In addition to reducing modulation spectral efficiency, system-synchronization to packet-level achieved by offset marker bit-spacing is difficult over long fiber spans due to Gordon–Haus induced timing jitter [56] and the requirement of current all-optical regeneration architectures (i.e., [18], [19]) for fixed bit-period spacing to achieve successful regeneration of the incoming data format.

In this paper, we describe an ultrafast synchronous OTDM network testbed [52]–[54] that includes a headend, transmitter, and receiver passively connected to a continuous optical bus shown in Fig. 3. The headend generates the global clock and the time slots used to partition transmitted data. An actively mode-locked fiber laser tuned to 1550 nm in the headend generates the system clock which consists of 2 ps pulses at a 12.5 GHz repetition rate. In order to mark the beginning of each 100 ns long OTDM slot, an electro-optic modulator removes one of every 1250 clock pulses. The headend continuously launches the empty slots shown in Fig. 3 onto the system bus.

The transmitter generates a network address header and data payload and inserts both into an empty network slot on the system bus. It should be noted that our slot synchronization and address comparison technique is designed to work for serial 100 Gb/s random data. In our current demonstration, however, we use bit-interleaving techniques as a cost-effective method to generate high-speed pseudorandom binary sequence (PRBS) data for insertion into OTDM slots. The transmitter passively taps a portion of the energy from the system bus and modulates the coupled clock pulses via PPM into a 4-bit network address header and PRBS data payload. PPM data formatting is used to mitigate pattern-dependent-gain-saturation-induced amplitude patterning in the semiconductor-based UNI optical logic gates. This 12.5 Gb/s packet is then optically multiplexed to 100 Gb/s and passively coupled and interleaved with the 12.5 GHz clock pulses in the network slot on the system bus to achieve the 112.5 Gb/s line rate shown in Fig. 4. In the multiplexer, optical delays $7T/9$, $10T/9$, and $14T/9$ (where $T = 80$ ps is

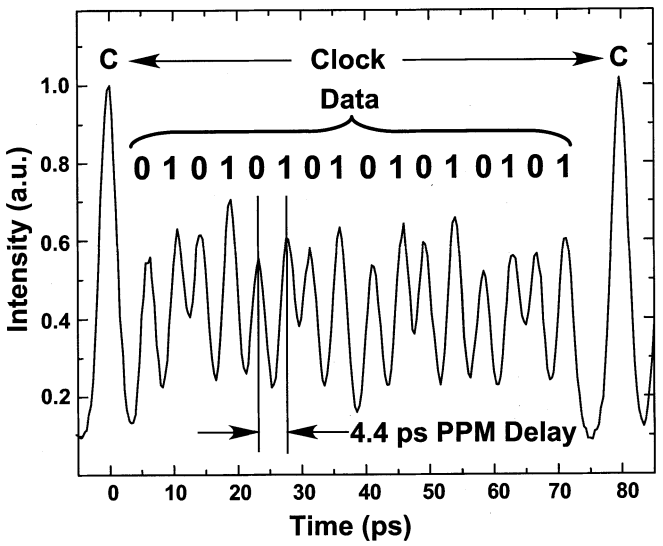

Fig. 4. Optical cross correlation of the transmitter output showing 112.5 Gb/s system rates (100 Gb/s PPM data with 12.5 Gb/s clock). The clock pulses appear twice as intense as the data pulses due to the 50% mark-to-space ratio imposed on the pseudorandom binary sequence data.

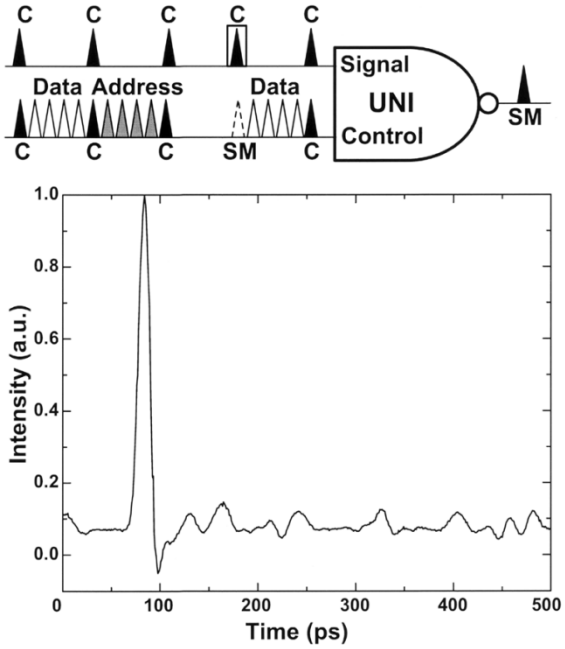

Fig. 5. Slot marker detection functional block diagram and measured digital sampling oscilloscope trace. The global clock and local receiver clock pulses (C) are temporally aligned at the UNI and the missing SM pulse opens an optical switching window in the signal pulsetrain which outputs a single SM pulse from the UNI. The digital sampling oscilloscope trace indicates the SM detection process is achieved with a 8.5-dB extinction ratio.

the bit period at 12.5 Gb/s) are used to decorrelate adjacent bits after multiplexing and provide an opening in each bit-period for global clock insertion. The 112.5 Gb/s OTDM line rate exceeds electronic processing speeds. Therefore, optical cross-correlation with 2 ps sampling pulses at 12.5 Gb/s is used to image the 112.5 Gbit/s OTDM slot in Fig. 4. If multiple transmitters are on the network, a determination of whether or not a slot is empty or full must be made before a given transmitter attempts to fill the slot with its own data. Because PPM data results in a pulse in every bit period, the empty slot energy will be lower than a full slot and empty/full slot determination is conceptually simple. Because global clock pulses are modulated in the transmitter, the need for a local optical source is eliminated, thus extending network scalability and achieving self-synchronization between the transmitter address header/data payload and headend-generated slot.

The receiver passively taps a fraction of the energy from the system bus. The coupled network pulse train is then optically amplified and directed to three all-optical logic gates that perform slot marker detection, address comparison, and data rate downconversion in order for electronic processing of the payload to occur as shown in Fig. 3. In our OTDM system receiver, each all-optical logic gate shown in Fig. 3 is a UNI. The incoming network pulse train at the slot marker (SM) detection UNI is timed via τ_1 in Fig. 3 so that the global clock pulses and slot marker are temporally aligned with the locally generated optical pulse train composed of 2 ps pulses at a rate of 12.5 GHz and a center wavelength of 1545 nm. Bit-phasing between the network and local receiver pulse trains is maintained using an optoelectronic dithering phase-locked loop. When used as an optical logic gate, the control and signal pulse trains are bit-wise compared with the Boolean logical function designed into the UNI and the result is output on the signal pulse train wavelength. The slot marker detection UNI is configured to perform a logical NAND function which results in a single pulse output that occurs for every absent slot marker pulse on the incoming network pulse train. Because this UNI is biased as a NAND gate, a single signal pulse at 1545 nm is switched out of the gate only when the missing slot marker pulse is present in the control stream at the UNI. This single pulse provides a temporal marker local to the receiver that signifies the beginning of a slot. Although this technique is adaptable to variable-length packets, we used a fixed 100 ns long slot size in our experiment. In the 100 Gb/s OTDM system, optimal slot marker detection is achieved with a 2.5 ps switching window and switching energies less than 25 fJ. As shown in Fig. 5, an extinction ratio of 8.5 dB is achieved for the slot marker detection process with 7 fJ signal and 24 fJ control pulse train UNI switching energies. We recognize that spectral efficiency is reduced using this slot timing synchronization technique. Aggregate data rates of 1.28 Tb/s have been demonstrated for a single OTDM channel [55], however, and the inclusion of a 12.5 GHz global clock in this case results in only a 1% reduction in spectral efficiency. This single pulse defines a reference for the beginning of the OTDM slot at the receiver that is insensitive to variable propagation delays on the system bus due to timing jitter and polarization-mode dispersion in the optical fiber channel separating the transmitter and receiver in the OTDM network.

All-optical address comparison is achieved at the UNI biased to perform the Boolean AND function shown in Fig. 3. In this optical logic gate, the local receiver address is temporally aligned via τ_2 to overlap one of the 12.5 Gb/s interleaved network packet address channels. The local address is generated from the single slot marker reference using standard optical multiplexing methods [46]. In this experiment, the local receiver address [1001] is generated in the PPM format with a 4.4 ps PPM delay as shown in Fig. 6. The network slot ad-

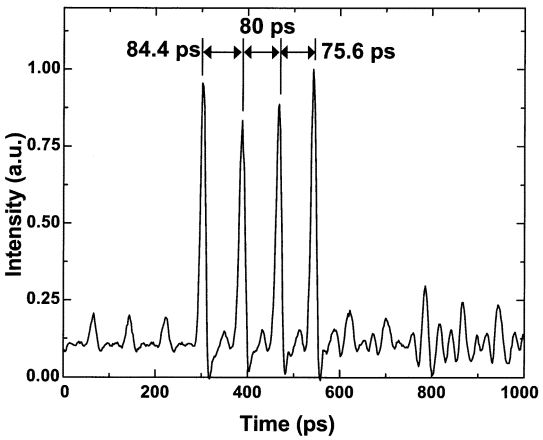

Fig. 6. Digital sampling oscilloscope trace showing the local receiver optical address generated from the single slot marker pulse. The address corresponds to [1001] with a pulse position modulation delay of 4.4 ps.

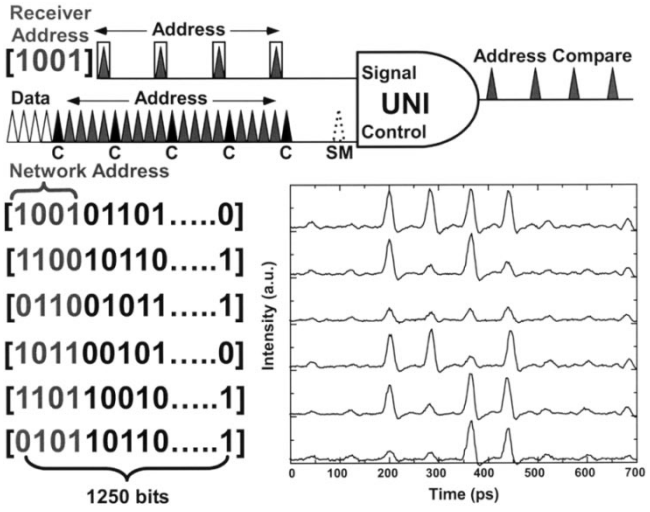

Fig. 7. Address comparison functional block diagram and experimental results. One 12.5 Gb/s bit-interleaved channel in the network slot address and the local receiver address are temporally aligned and bit-wise compared at the ultrafast nonlinear interferometer (UNI) with complementary Boolean XOR functionality. The digital sampling oscilloscope trace indicates the address comparison results for six distinct network addresses that is achieved with a 6.4 dB extinction ratio.

dress is generated in this example by setting the pattern generator to create a 1250-bit slot consisting of repeating copies of the [100 101 101] unit-cell such that 138 copies of the unit-cell plus eight remaining bits are contained in each slot. This technique results in a 4-bit network slot address which changes from slot-to-slot by one sequential bit in the 9-bit unit-cell creating 7 distinct addresses (i.e., [1001], [1100], [0110], [1011], [1101], [0101], and [0010]). Each network slot address is then bit-wise compared to the local receiver address at the UNI biased for AND operation as shown in Fig. 7. The address comparison UNI is optimized to perform a logical AND function with a 2.5 ps switching window and switching energies less than 20 fJ. An extinction ratio of 6.4 dB is achieved between matched and unmatched address bits for the address comparison with 1 fJ signal and 19 fJ control pulsetrain UNI switching energies. This address comparison is scalable to OTDM slots with high-speed serial data because the UNI is capable of 100 Gb/s bitwise logic [27]. It should be noted that the UNI is shown to be stable over time periods longer than one hour because each logic gate was biased for operation and untouched during the collection of all data shown in Fig. 7. In addition, the address-space is scalable and can be fully utilized because keyword comparison [50] is not required. Finally, an important feature of this address-comparison technique is that complementary Boolean XOR logic is achieved from an optical AND gate because each address is generated using the PPM format in which a pulse is present for both logical "0"s and "1"s. Therefore, when either a "0" or "1" address match is detected, the UNI outputs a pulse and an address match is verified in this example when four optical pulses are output from the address comparison UNI in Figs. 3 and 7.

The output of the optical address comparison gate is processed by a high-speed 4-input AND gate to determine whether or not all of the address pulses match. If an address match between the local receiver and network header is determined, the "1" output from the 4-input AND gates the error detector in Fig. 3 for the 100 ns OTDM network slot length. The data input into the error detector is provided by optically demultiplexing one of the eight 12.5 Gb/s PRBS data sequences from the OTDM slot payload and by converting the data format from PPM to on-off keying using the demultiplexer UNI shown in Fig. 3. If an address mismatch between the local receiver and network header is determined, the slot payload is intended for a different receiver on the network and the "0" output from the 4-input AND gate leaves the error detector in the inactive state.

The final optical logic gate in the OTDM network testbed shown in Fig. 3 is the demultiplexer. At present, we have demonstrated all-optical demultiplexing of PPM data at rates up to 80 Gb/s [57]. The reason that we have demonstrated 80 Gb/s instead of 100 Gb/s as required for the current testbed is that these experiments were performed at SONET standard rates which consist of 10 Gb/s and 40 Gb/s channel rates. Our 1:8 multiplexer, therefore provided a top data rate of 80 Gb/s for the experiments presented in this section. Work is currently underway to demonstrate all-optical demultiplexing of 100 Gb/s PPM data in the OTDM testbed. Our experimental setup for demultiplexing with the UNI is shown in Figs. 8 and 10. In Fig. 8, the data at the aggregate OTDM rate of 80 Gb/s is used as the signal input to the UNI. Control pulses at 10 GHz gate the incoming signal data, routing every eighth pulse to the output of the switch. The UNI is designed to provide a switching window duration of 5 ps. Because the switching window duration is less than the 6.25-ps PPM offset, the control pulses may be temporally aligned to gate exclusively the "1"s in the overlapped channel of the aggregate OTDM data, thus providing a format conversion to 10 Gb/s OOK modulation at the output of the demultiplexer. A longer switching window could be used to maintain the PPM format.

The results of bit-error rate (BER) tests performed at the attenuated output of the switch using a 10 Gb/s OOK optically preamplified receiver are shown in Fig. 9. The baseline is measured using the OOK data directly from one of the arms in the PPM modulator shown in Fig. 2. The control pulse and signal pulse energies in the demultiplexing experiments were maintained at 500 fJ and 12.5 fJ, respectively. For aggregate PPM data rates up to 40 Gb/s a maximum power penalty of 1.2 dB

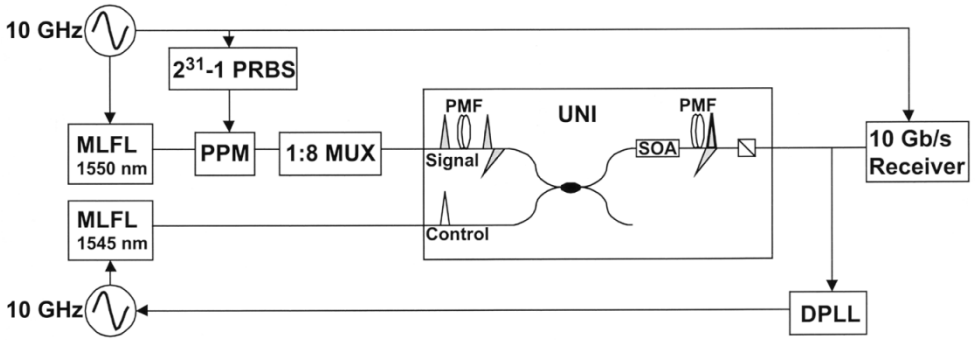

Fig. 8. Experimental setup for demultiplexing of data on signal input of UNI. MLFL: Mode-locked fiber laser. PPM: Pulse-position modulator. PMF: Highly birefringent polarization-maintaining fiber. DPLL: Dithering phase-locked loop.

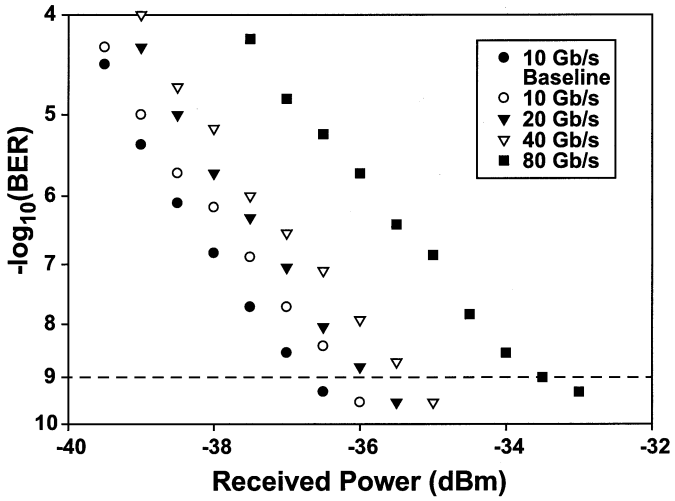

Fig. 9. Bit-error rate (BER) performance for demultiplexing from aggregate PPM data rates of 10, 20, 40, and 80 Gb/s on signal input to UNI.

at a BER of 10^{-9} is observed. This penalty is largely due to the wavelength selectivity of the receiver and the imperfect contrast of the demultiplexer. The larger power penalty of 3 dB observed at 80 Gb/s is due to intersymbol interference (ISI) in the UNI. This penalty arises because signal pulses in the UNI are split into orthgonally polarized pairs, temporally separated by 5 ps, by the birefringent fiber. Because of the PPM data format, pulses in the data stream may be separated by as little as 6.25 ps. Thus, adjacent pulse overlap may occur in the UNI leading to the observed ISI. This effect may be mitigated by reducing the length of birefringent fiber in the UNI, thereby reducing the temporal separation of the signal pulse pairs in the SOA.

Because the use of PPM data reduces gain-saturation induced patterning in the UNI, demultiplexing may also be performed with data at the aggregate rate (80 Gb/s) used as the control input to the UNI [57] as shown in Fig. 10. In this configuration, the UNI acts as a wavelength converter, converting every eighth control pulse to the signal wavelength. As in the previous demonstration, signal and control pulses are provided at 10 GHz repetition rates by two mode-locked fiber lasers producing 2 ps pulses at 1550 and 1545 nm. The control pulses are modulated with a PPM data pattern. To demonstrate the pattern-independent operation of the switch, a long data pattern of length $2^{31}-1$ is used. The PPM data is then passively multiplexed to rates of 10, 20, 40, and 80 Gb/s and input to the control port of the UNI. As in the first demonstration, the UNI switching window duration of 5 ps provides a format conversion from PPM to OOK at the output of the UNI. In this setup, maintaining the PPM data format at the output of the switch would require splitting each signal pulse into two pulses separated by the PPM offset.

The results of bit-error rate tests at the output of this demultiplexer are shown in Fig. 11. Error-free operation ($\mathrm{BER} < 10^{-9}$) is obtained for all aggregate data rates with control and signal pulse energies of 25 fJ and 12.5 fJ, respectively. Because the signal pulses are at the demultiplexed rate, the contrast ratio of the demultiplexer between signal pulses is not as important in this experiment as in the first demultiplexing experiment. Thus, good performance is obtained with significantly reduced control pulse energies. For aggregate control pulse data rates of up to 40 Gb/s a small power penalty of < 0.5 dB from baseline is observed. At 80 Gb/s the power penalty of 2 dB is thought to be a result of the increased saturation of the SOA due to the high average power of the control pulses.

Polarization sensitivity is an important issue that we have considered in the design of our slotted OTDM receiver. The UNI gate configuration exploits nonlinearities in the SOA to rotate the signal pulse polarization and achieve ultrafast switching. The polarization sensitivity of the UNI to signal and control inputs shown in Fig. 1, however, are not equivalent. The primary source of polarization sensitivity in the UNI is the signal input because the signal pulse polarization must be carefully aligned to the birefringent fiber to produce equal amplitude, temporally separated orthogonal pulse components inside the switch. Sensitivity to the control pulse polarization is minimal because the nonlinearity induced in the SOA is largely due to control pulse saturation of the carrier density and we use commercial SOAs with gain polarization dependence $<$1 dB. In order to minimize the polarization sensitivity of our OTDM receiver, we direct the locally generated fixed-polarization receiver clock into the polarization-dependent signal inputs and the uncontrolled-polarization 100 Gb/s network data into the polarization-independent control inputs of the slot marker, address comparison, and demultiplexer UNIs shown in Fig. 3.

We have demonstrated a slotted OTDM multiaccess network testbed capable of operating at 112.5 Gb/s line rates. A headend provides global network timing and slot definition. The transmitter generates a scalable address header and 100 Gb/s

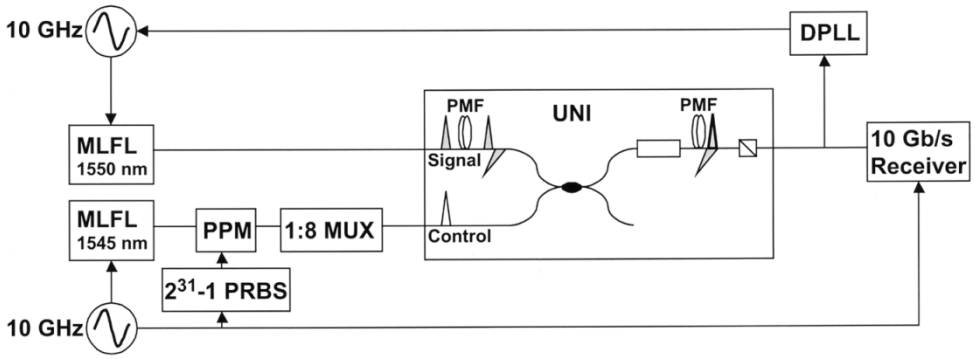

Fig. 10. Experimental setup for demultiplexing of data on control input of UNI. MLFL: Mode-locked fiber laser. PPM: Pulse-position modulator. PMF: Highly birefringent polarization-maintaining fiber. DPLL: Dithering phase-locked loop.

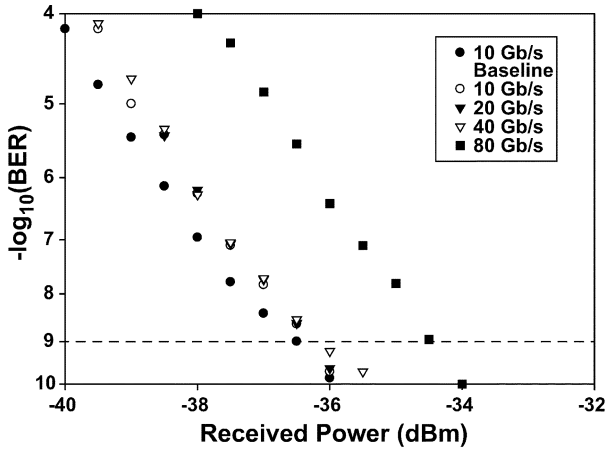

Fig. 11. Bit-error rate (BER) performance for demultiplexing from aggregate PPM data rates of 10, 20, 40, and 80 Gb/s on control input to UNI.

pseudorandom data payload using pulse-position modulation signaling format. The receiver achieves self-synchronization to slot timing, address comparison, and data rate downconversion using three cascaded all-optical logic gates operating at the 112.5 Gb/s network line rate. For the experiments presented in this section, the transmitter and receiver in our OTDM testbed were separated by only a few tens of meters of optical fiber. For a true local area network demonstration, an OTDM system must be able to operate with network node separations up to 100 km.

IV. Long-Haul Transmission

During the past year, we have begun to investigate transmitting high-speed OTDM data over significant distances of fiber as required in wide area third-generation packet-switched network applications. Our ultimate goal is to successfully transmit and receive OTDM data over BoSSNET [58], an installed East Coast fiber optic link operated by MIT Lincoln Laboratory, at single-channel rates of 160 Gb/s and beyond. We discuss here some of the challenges to transmitting short-pulses over fiber and report some of our recent results.

For long-haul transmission at speeds up to 40 Gb/s, soliton transmission systems and dispersion managed soliton systems have been used to successfully transmit data over long distances. Although recent theoretical research suggests that there is the potential for extending dispersion-managed soliton systems to speeds as high as 160 Gb/s and beyond, these systems will likely require very dense dispersion management which could limit their applicability with currently installed fiber [59], [60]. To date, most of the reported transmission experiments at 160 Gb/s and higher have used quasilinear transmission in which the path-averaged dispersion is close to zero and the dominant nonlinear effect is intrachannel four-wave mixing [61], [62]. Because we plan to eventually transmit data on a previously deployed in-the-ground fiber infrastructure, we have chosen to use quasilinear transmission with accurate dispersion compensation at the access points. We believe that this approach in combination with optical regeneration, is one of the most promising avenues toward a 160 Gb/s OTDM network.

In the quasi-linear regime, a significant impairment to short pulse propagation in optical fiber is intersymbol interference. Two significant sources of intersymbol interference are incomplete dispersion compensation and nonlinear intrachannel interference. The most commonly used dispersion compensation technique is to balance second order dispersion accumulated in a transmission fiber span by a length of fiber with the opposite dispersion. While dispersion management is widely used in conventional WDM systems, the amount of dispersion that can be tolerated in an OTDM system is much smaller than for a WDM system of the same capacity. OTDM systems transmit data using short optical pulses with durations on the order of 1–3 ps. High data rates are then achieved by packing the data pulses as closely together as possible. Because the pulses are closer together less temporal broadening can be tolerated due to uncompensated residual dispersion in the transmission fiber span before intersymbol interference limits system performance.

The dispersion map for our transmission experiment consisted of 100 km of Corning LEAF® fiber with a dispersion of 4.1 ps/nm · km followed by a dispersion compensation module comprised of 3.2 km of dispersion compensation fiber. Fig. 12 plots the measured total dispersion of the 100 km span of LEAF® transmission fiber and the dispersion compensation fiber. The dispersion compensation module used in this paper was specifically tailored to eliminate both the dispersion and dispersion slope. The resulting total dispersion (plotted in the middle curve) reaches 0 at a wavelength of 1547.4 nm with a dispersion slope of 3.6 ps/nm^2.

The small residual dispersion slope would not pose a significant problem for a WDM system, however in an OTDM system

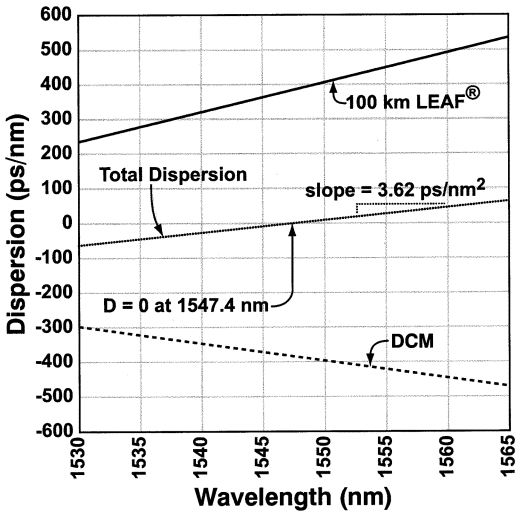

Fig. 12. Measured dispersion for a 100 km span of Corning LEAF® fiber (top curve), dispersion compensation module (bottom curve), and the total dispersion of both (center curve).

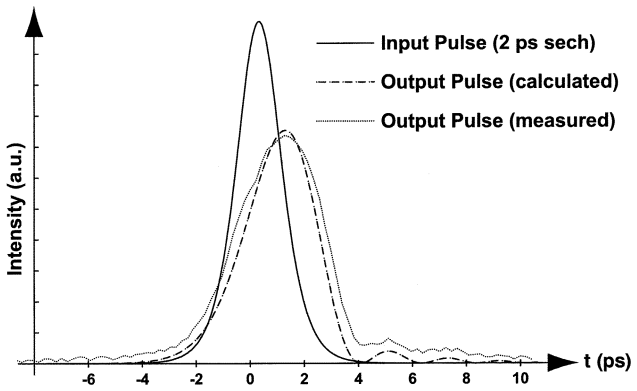

Fig. 13. Calculated and measured pulse distortion after propagation over 100 km of fiber with dispersion compensation. Third-order dispersion (dispersion slope) causes the observed oscillations on the trailing edge of the pulse.

the dispersion slope can lead to significant pulse distortion, even when the center wavelength is adjusted to the zero-dispersion point [63], [64]. Fig. 13 shows the calculated and measured pulse shape for 2 ps pulses transmitted over the compensated span represented earlier in Fig. 12. Because of the limited speed available with optical detectors, the pulses were measured using a nonlinear optical sampling cross-correlator, in which the pulse is sampled by a comparatively short optical pulse in a nonlinear medium. The oscillations seen on the trailing edge of the pulse are characteristic of third-order dispersion. This effect can cause pulses to spill over into neighboring bit slots, leading to inter-symbol interference. For longer propagation distances or higher bit-rates, fourth-order dispersion will also prove to be significant.

In order to extend the propagation distance and mitigate time-varying dispersion in a wide area OTDM network, more accurate and possibly tunable dispersion compensation systems will be needed. One technique is to use tailored Bragg gratings to match the dispersion of a span [65]. Fiber Bragg gratings can also be mechanically stressed to provide a tunable device capable of compensating third order dispersion [66]. Another technique that is capable of providing exact tunable compensation for even-ordered dispersion components can be implemented with a phase-conjugating medium inserted at the midpoint of the span, which causes the second half of the span to undo the dispersion experienced in the first half [67]. Another promising approach is to prechirp the input pulses in order to compensate for any residual dispersion in the span [68]. This technique is capable of tunable dispersion compensation by feedback control on the drive voltage into the prechirp phase modulator. Finally, new and improved dispersion compensation fiber is being aggressively researched, and some research groups have achieved high-speed transmission by alternating spans of conventional fiber with reverse dispersion fiber that is specifically engineered to have a dispersion profile opposite to that of conventional fiber.[69] This approach, however, does not provide tunable dispersion compensation and may be challenging to apply in currently deployed fiber systems where the span lengths and fiber types have been preselected.

Nonlinearity in the optical fiber can also be a significant impairment for short-pulse communication systems. In WDM systems, one of the most significant nonlinear effects is four-wave mixing, in which the nonlinear mixing of adjacent WDM channels leads to a crosstalk penalty, see for example [70]–[73]. By contrast, in single-channel OTDM systems the dominant effect is interpulse cross-phase modulation (XPM), see for example [64], [74]–[79]. The short-pulses in an OTDM data stream disperse very quickly in optical fiber, spreading into many adjacent timeslots before the original pulse sequence is restored by dispersion compensation. During the time when the pulses overlap, nonlinear effects can cause the pulses to mix with each other, which can lead to random fluctuations in the pulse amplitudes. It has been shown that intersymbol interference due to nonlinear pulse overlap is a strong function of the dispersion magnitude in the transmission and compensation fiber spans [74].

Fig. 14 presents the measured performance in our initial experiments with OTDM transmission. In these experiments, the data was transmitted over 100 km of LEAF® fiber with dispersion compensation and an intermediate amplifier after 50 km. The input pulses were generated by a mode-locked fiber laser, which produced transform-limited 2 ps pulses at a repetition rate of 12.5 GHz. The average power input to the transmission fiber was 10 mW and the pulse train center wavelength was 1547.4 nm. We tested both OOK and PPM data format transmission. The pulses were passively multiplexed to single-wavelength channel rates up to 50 or 100 Gb/s for PPM and OOK data transmission, respectively. At the receiver, the pulses were demultiplexed to 12.5 Gb/s using an ultrafast nonlinear interferometer [57]. As an interim solution to the problem of clock recovery, we used a separate wavelength channel to transmit a 12.5 GHz clock tone along with the data signal. At the receiver, the clock tone was spectrally filtered from the data, and routed to a conventional low-speed phase-locked loop clock recovery system. For data rates up to 50 Gb/s, the data in Fig. 14 shows no appreciable power penalty for transmission over 100 km compared to back-to-back measurements. When transmitting 100 Gb/s data using on-off keying, a significant power penalty and error floor is present. We believe both system impairments can be attributed to intersymbol interference at the receiver due to residual uncompensated third-order dispersion in the transmis-

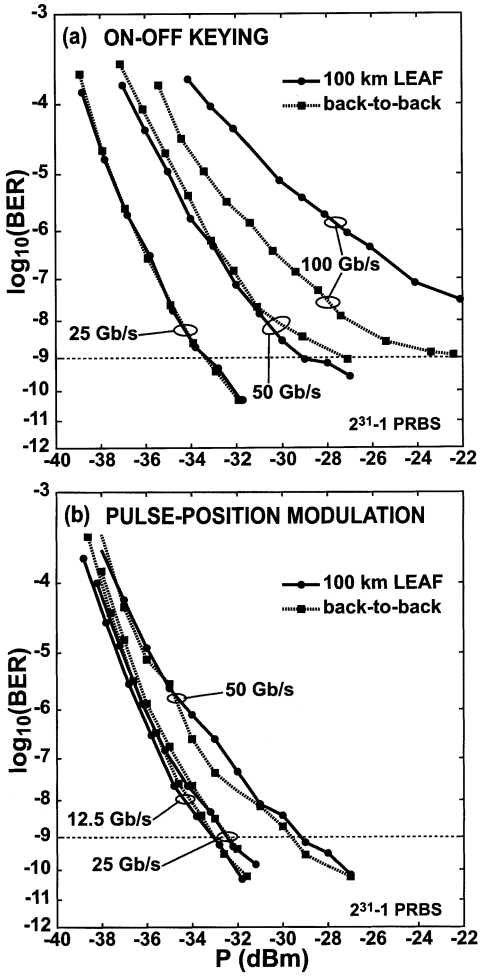

Fig. 14. (a) Measured bit-error rate performance for long-haul transmission of on-off keyed OTDM data at rates up to 100 Gb/s. (b) Measured bit-error rate performance for long-haul transmission of pulse-position modulated OTDM data at rates up to 50 Gb/s.

sion fiber span and intersymbol interference in the UNI demultiplexer when aggregate OTDM data is input to the signal port.

V. All-Optical Regeneration

In order to overcome the transmission penalties incurred by chromatic dispersion and fiber nonlinearities during short optical pulse propagation over long distances, the network data pulse train can be periodically regenerated. In WDM systems, regeneration of a distorted optical signal is achieved by converting to an electronic signal, demultiplexing the data to many lower rate streams for parallel processing, followed by remultiplexing to a high-rate electronic signal that is then remodulated onto the desired optical carrier. In OTDM systems, the use of short optical pulses makes possible 3R regeneration in which the data pulse train is reamplified, reshaped, and retimed using all-optical techniques. The key components of an all-optical 3R regenerator are a local optical pulse source, clock recovery to synchronize the network and local pulse trains, and an ultrafast optical switch that is used to replace the distorted network pulses with transform-limited optical pulses generated in the regenerator.

A critical challenge in all-optical 3R regeneration is clock recovery. In order for a regenerator to successfully operate, it must have an electrical clock signal that is synchronized with the incoming optical data from a remote location. Several techniques have been developed to perform optical clock recovery including resonant oscillator circuits [80], injection locking of pulsed sources [81], and phase-locked loops [82]. Of these three, phase-locked loops are one of the more flexible techniques.

The critical element of a phase-locked loop is the phase detector, which compares the phase of the local clock signal with the incoming data. Electrical phase-locked loops use a conventional electronic mixer to compare the phase of a local oscillator to the incoming data, and they are therefore limited by the operating speed of mixers and photodetectors. Some improvement can be gained by using an electrooptic modulator or an electroabsorption modulator to compare the phases. In this approach, a locally generated electrical clock signal drives an optical modulator that modulates the optical data signal. The emerging optical signal can be detected with a relatively slow photodiode to measure the phase difference [83], however these devices are instead limited by the switching speed of the modulators. To overcome this limitation, one must use an optical phase detection method, in which both the local clock and the incoming data are optical signals that interact in a nonlinear medium. Researchers at NTT use four-wave mixing either in an SOA or optical fiber to provide the nonlinear mixing between the clock and the data [84]. We currently use a UNI in a dithering phase-locked loop to correct for phase-drift between the incoming data and the local clock signal. This system can correct for slow phase drifts, but it currently relies upon an external electrical connection to provide frequency synchronization. We are currently investigating alternative clock recovery schemes that can acquire both phase and frequency.

All-optical pulse regeneration has been demonstrated previously in the nonlinear optical loop mirror [24], ultrafast nonlinear interferometer [18], polarization-discrimination symmetric Mach–Zehnder [19], Mach–Zehnder interferometer [85], delayed interference signal converter [86], Michelson interferometer [87], and electroabsorption modulator [88]. As discussed previously, semiconductor-based switches offer advantages over fiber-based switches due to the large nonlinear response of the semiconductor. However, carrier dynamics in the semiconductor can have deleterious effects on an optical signal (e.g., from ASE or pattern-dependent gain saturation) which may be unsuitable for regenerator applications. For these applications, optical fiber, with its ultrafast nonlinear response ($<$10 fs), may provide a more suitable nonlinear medium. The relatively small nonlinear response of an optical fiber requires a long interaction length ($\sim$1-5 km) in fiber-based switches. However, the associated latency of these switches may not be important in applications such as all-optical regeneration where processing of the signal after the switch is not required. A significant challenge for fiber-based switches is polarization instability caused by temperature fluctuations and acoustic effects in the fiber. One solution, which has been applied to the nonlinear optical loop mirror, is passive polarization stabilization using a Faraday mirror [89]. Here, we present an all-optical regenerator based on the UNI which uses a dispersion shifted fiber as the nonlinear medium, instead of an SOA. Polarization stabilization is achieved by Faraday rotation

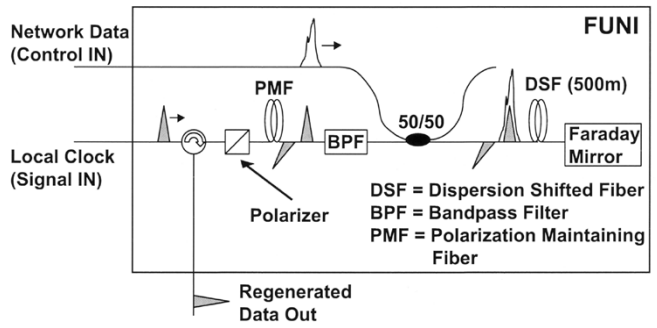

Fig. 15. Folded ultrafast nonlinear interferometer with Faraday mirror passive polarization stabilization configured to perform 3R all-optical regeneration.

in a switch configuration we call the folded ultrafast nonlinear interferometer (FUNI) [25], [30].

While the true benefits of all-optical regeneration are realized for operation on ultrafast data rate short-pulse trains, we demonstrate the viability of this switch stabilization technique for all optical regeneration of 2.5 ps pulses at 10 Gb/s using the FUNI shown in Fig. 15. A local clock source generates transform limited 2.5 ps pulses at 10 Gb/s. Incoming network data pulses switch local transform-limited clock pulses out of the FUNI. Optical regeneration is achieved because the clock pulses are modulated to match the bit pattern of the data pulses. At the signal input to the FUNI, the polarization of the clock pulses is set to be linear and pass maximally through the polarizer. A length of polarization maintaining birefringent fiber cross-spliced at 45° to the polarizer splits each clock pulse into two orthogonal components separated by 5 ps. A data pulse stream is coupled onto the fiber so that the data pulses are coincident with one of the two polarization components created when the clock stream passes through the polarization maintaining fiber. In the absence of data pulses, the clock pulses are reflected out of the polarizer. In the presence of data pulses, nonlinearities induced in the dispersion-shifted fiber produce a relative phase shift between the two clock pulse polarizations and they pass through the polarizer to the circulator port labeled "Regenerated Data Out."

Polarization stabilized operation of the FUNI shown in Fig. 15 is achieved using a Faraday mirror to mitigate the deleterious effects of birefringence in the fiber. Another attractive means of implementing a stabilized fiber switch is to use polarization maintaining fiber as the nonlinear medium [90]. This technique however, has a potential drawback: the high birefringence of the polarization maintaining fiber results in the two orthogonal clock pulse components temporally overlapping or "walking-through" multiple network data pulses during transmission through the device. This polarization maintaining fiber induced walk-through causes an unpredictable phase-shift due to network data pattern dependence as well as a degraded switch output contrast. In contrast, group velocity dispersion is nearly zero around 1550 nm in dispersion-shifted fiber and the clock and data pulse train wavelengths in the FUNI can be adjusted to alter the total walk-through to be a few picoseconds. In this case, a few picosecond "walk-through" slightly widens the FUNI switching window which helps to correct timing jitter on the incoming network data pulse train.

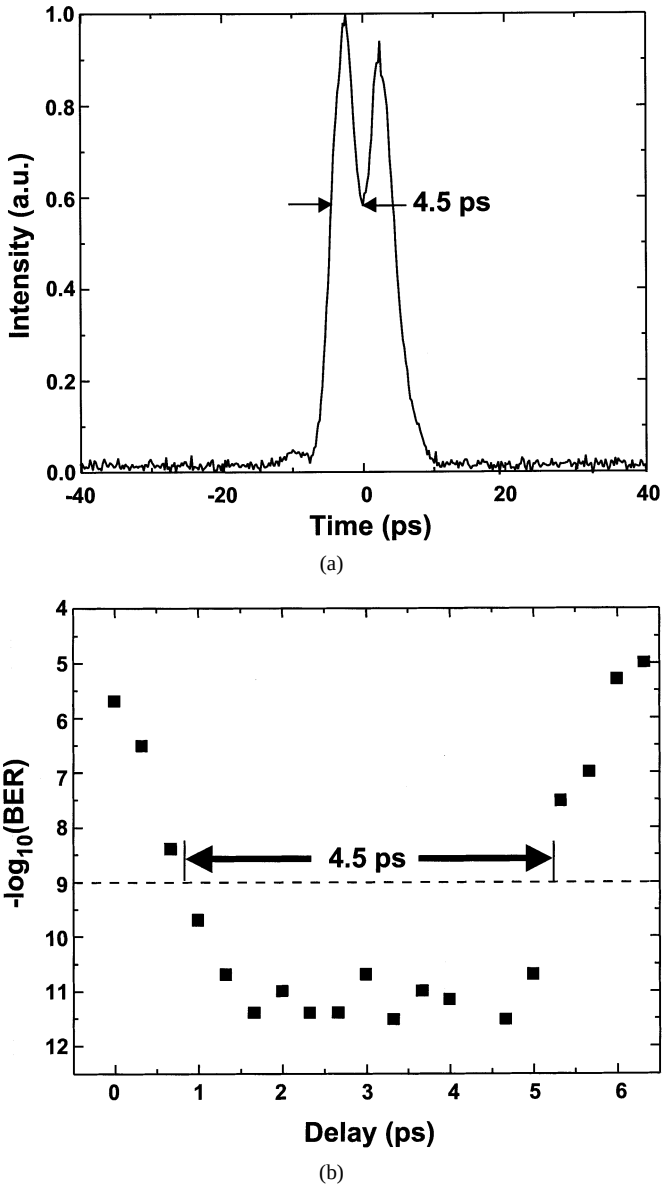

Fig. 16. (a) The folded ultrafast nonlinear interferometer (FUNI) switching window has a double peak shape and 4.5 pulsewidth. (b) The FUNI when used for 3R regeneration provides error-free operation ($\mathrm{BER} < 10^{-9}$) for up to 4.5 ps of timing jitter between the network data and local clock pulses.

The FUNI switching window is shown in Fig. 16(a) and the corresponding tolerance to network data timing jitter is shown in Fig. 16(b). From these figures, the FUNI switching window width is related to the amount of timing jitter the device can compensate. By adjusting the dispersion shifted fiber length and the local clock pulse train wavelength, the FUNI switching window width can be adjusted. The FUNI switching window shown in Fig. 16(a) contains two peaks spaced by 5 ps because a network data pulse in the regenerator can temporally overlap either of the two orthogonal clock pulse components separated by 5 ps. We used a 500 m length dispersion-shifted fiber, 1545 nm network data wavelength, and 1555 nm regenerator clock wavelength in the FUNI to achieve a 4.5 ps switching window width for a single peak shown in Fig. 16(a).

In order to verify that the FUNI jitter tolerance is approximately equal to the switching window single-peak full-width at

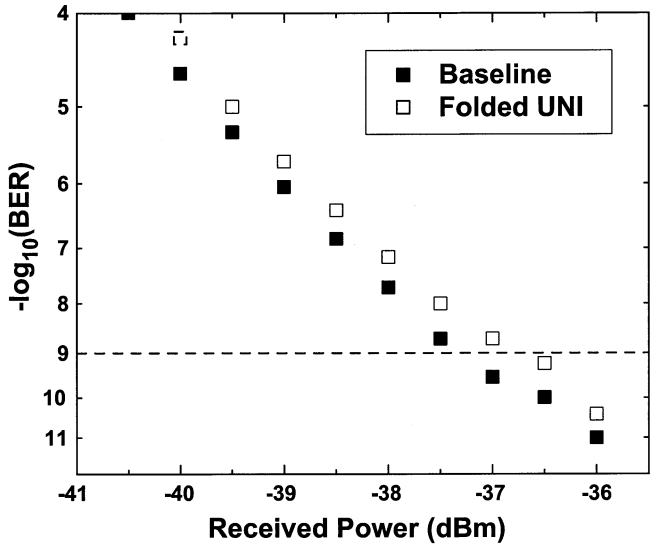

Fig. 17. Folded UNI bit error rate test (open squares) compared to reference back-to-back measurement (solid squares) for $2^{31}-1$ pattern length on-off keyed data at 10 Gb/s. The power penalty between the baseline and the FUNI at an error rate of 10^{-9} is 0.5 dB.

half-maximum, the network data was regenerated onto the local clock wavelength and set at a 10^{-11} error rate. A manual optical time delay in the local clock pulse train path was used to simulate timing jitter between the clock and data. Fig. 16(b) verifies that the FUNI timing jitter tolerance is 4.5 ps for error-free operation ($\mathrm{BER} < 10^{-9}$), as predicted from the switching window width, for a received optical power of -32 dBm network data pulse energy, and 660 fJ local clock pulse energy.

To verify that the 3R regenerated FUNI output is undistorted after processing by the switch, the bit-error rate characteristic is measured as a function of the optical power into a preamplified 10 Gb/s receiver. The network data consists of a $2^{31}-1$ length pseudorandom bit-pattern modulated onto a 10 GHz repetition rate optical pulse train at 1545 nm. The local regenerator clock consists of a 10 GHz repetition rate optical pulse train at 1550 nm. In this experiment, the network data pulse energy was 4.6 pJ and the local regenerator clock pulse energy was 170 fJ. The results of the bit-error rate test are shown in Fig. 17. The baseline is measured by sending the 10 Gb/s network data directly into the preamplified receiver without the FUNI regenerator. We believe that the small 0.5 dB power penalty incurred at a bit-error rate of 10^{-9} is caused by the small gain ripple present in the receiver optical preamplifier between the regenerator clock and network data wavelengths.

Our 10 Gb/s results indicate that the folded UNI is capable of providing 3R regeneration in an all-optical network. Because the FUNI is implemented using dispersion-shifted fiber and a Faraday mirror, the switch architecture provides both inherent polarization stability and a tunable switching characteristic. We have demonstrated that the FUNI can achieve 3R regeneration of 2.5 ps optical pulses with minimal switch-induced distortion and a tolerance to network data timing jitter of up to 4.5 ps while still maintaining error-free operation. Due to the short switching window width < 5 ps, we believe this device should be capable of operation at single channel rates beyond 100 Gb/s.

VI. Conclusion

In this paper, we present ultrafast slotted optical time-division multiplexed networks as a viable means of achieving a highly capable next-generation all-optical packet-switched network which provides simple network management, the ability to support variable quality of service, self-routing of packets, scalability in the number of users, and the use of digital regeneration, buffering, and encryption. We have discussed the ultrafast nonlinear interferometer semiconductor-based optical logic gate which uses efficient cross-phase modulation to achieve bitwise logical operation at data rates in excess of 100 Gb/s. We have demonstrated a slotted OTDM multiaccess network testbed capable of operating at 112.5 Gb/s line rates. In this system, a headend generates a 12.5 Gb/s global clock and defines the 100 ns system slot boundaries. The transmitter generates a 4-bit address header and 100 Gb/s pseudorandom data payload using pulse-position modulation signaling format. The receiver achieves self-synchronization to slot timing, 4-bit address comparison, and data rate downconversion using three cascaded all-optical logic gates operating at the 112.5 Gb/s network line rate. Long-haul propagation of short optical pulses has also been investigated and we have shown that 2.5 ps wide 100 Gb/s OOK and PPM pulsetrains can be successfully transmitted over 100 km distances. Finally, we have investigated 3R all-optical regeneration as a viable cost-effective means of extending the long-haul distance of our OTDM network to distances much greater than 100 km.

Acknowledgment

The authors would like to thank Dr. T. G. Ulmer and Dr. W. E. Keicher for helpful discussions and C. Demers for technical assistance provided during this work.

References

[1] D. Cotter, J. K. Lucek, and D. D. Marcenac, "Ultra-high-bit-rate networking: From the transcontinental backbone to the desktop," *IEEE Commun. Mag.*, vol. 35, pp. 90–95, Apr. 1997.

[2] B. Y. Yu, P. Tolliver, R. J. Runser, D. Kung-Li, D. Zhou, I. Glesk, and P. R. Prucnal, "Packet-switched optical networks," *IEEE Micro*, vol. 18, pp. 28–38, Jan.-Feb. 1998.

[3] S. G. Finn, "HLAN—An architecture for optical multi-access networks," *Tech. Dig. LEOS Summer Top. Meeting*, vol. 45, 1995.

[4] R. A. Barry, V. W. S. Chan, K. L. Hall, E. S. Kintzer, J. D. Moores, K. A. Rauschenbach, E. A. Swanson, L. E. Adams, C. R. Doerr, S. G. Finn, H. A. Haus, E. P. Ippen, W. S. Wong, and M. Haner, "All-optical network consortium—Ultrafast TDM networks," *IEEE J. Select. Areas Commun.*, vol. 14, pp. 999–1013, June 1996.

[5] V. W. S. Chan, K. L. Hall, E. Modiano, and K. A. Rauschenbach, "Architectures and technologies for high-speed optical data networks," *J. Lightwave Technol.*, vol. 16, no. 12, pp. 2146–2168, Dec. 1998.

[6] A. Hasegawa and H. Toda, "A feasible all optical soliton based inter-LAN network using time division multiplexing," *IEICE Trans. Commun.*, vol. E81-B, no. 8, pp. 1681–1686, Aug. 1998.

[7] J. D. Moores, J. Korn, K. L. Hall, S. G. Finn, and K. A. Rauschenbach, "Ultrafast optical TDM networking: Extension to the wide area," *IEICE Trans. Commun.*, vol. E82-B, pp. 209–221, Feb. 1999.

[8] J. P. Sokoloff, P. R. Prucnal, I. Glesk, and M. Kane, "A terahertz optical asymmetric demultiplexer (TOAD)," *IEEE Photon. Technol. Lett.*, vol. 5, pp. 787–790, July 1993.

[9] T. Morioka, S. Kawanishi, H. Takara, and M. Saruwatari, "Multiple-output, 100 Gbit/s all-optical dumultiplexer based on multichannel four-wave-mixing pumped by a linearly chirped square pulse," *Electron. Lett.*, vol. 30, no. 23, pp. 1959–1960, Nov. 1994.

[10] M. Eiselt, W. Pieper, and H. G. Weber, "SLALOM: Semiconductor laser amplifier in a loop mirror," *J. Lightwave Technol.*, vol. 13, pp. 2099–2112, Oct. 1995.

[11] S. Nakamura and K. Tajima, "Ultrafast all-optical gate switch based on frequency shift accompanied by semiconductor band-filling effect," *Appl. Phys. Lett.*, vol. 70, no. 26, pp. 3498–3500, June 1997.

[12] B. S. Robinson, S. A. Hamilton, and E. P. Ippen, "Multiple wavelength demultiplexing using an ultrafast nonlinear interferometer," *Tech. Dig. Conf. Lasers and Electro-Optics*, vol. 56, 2001.

[13] T. G. Ulmer, M. Hanna, B. R. Washburn, S. E. Ralph, and A. J. SpringThorpe, "Microcavity-enhanced surface-emitted second-harmonic generation for ultrafast all-optical signal processing," *IEEE J. Quantum Electron.*, vol. 38, pp. 19–30, Jan. 2002.

[14] T. Durhuus, B. Mikkelsen, C. Joergensen, S. L. Danielsen, and K. E. Stubkjaer, "All-optical wavelength conversion by semiconductor optical amplifiers," *J. Lightwave Technol.*, vol. 14, pp. 942–954, June 1996.

[15] J. Leuthold, C. H. Joyner, B. Mikkelsen, G. Raybon, J. L. Pleumeekers, B. I. Miller, K. Dreyer, and C. A. Burrus, "100 Gbit/s all-optical wavelength conversion with integrated SOA delayed-interference configuration," *Electron. Lett.*, vol. 36, no. 13, pp. 1129–1130, June 2000.

[16] K. Tajima, S. Nakamura, and Y. Sugimoto, "Ultrafast polarization-discriminating Mach-Zehnder all-optical switch," *Appl. Phys. Lett.*, vol. 67, no. 25, pp. 3709–3711, Dec. 1995.

[17] S. Diez, R. Ludwig, and H. G. Weber, "Gain-transparent SOA-switch for high-bitrate OTDM add-drop multiplexing," *IEEE Photon. Technol. Lett.*, vol. 11, pp. 60–62, Jan. 1999.

[18] A. E. Kelly, I. D. Phillips, R. J. Manning, A. D. Ellis, D. Nesset, D. G. Moodie, and R. Kahsyap, "80 Gbit/s all-optical regenerative wavelength conversion using semiconductor optical amplifier based interferometer," *Electron. Lett*, vol. 35, no. 17, pp. 1477–1478, Aug. 1999.

[19] Y. Ueno, S. Nakamura, and K. Tajima, "Penalty-free error-free all-optical data pulse regeneration at 84 Gb/s by using a symmetric-Mach-Zehnder-type semiconductor regenerator," *IEEE Photon. Technol. Lett.*, vol. 13, pp. 469–471, May 2001.

[20] N. S. Patel, K. L. Hall, and K. A. Rauschenbach, "An all-fiber optical demultiplexer and XOR gate," in *Proc. SPIE*, vol. 2613, 1995, pp. 126–137.

[21] K. Uchiyama, T. Morioka, S. Kawanishi, H. Takara, and M. Saruwatari, "Signal-to-noise ratio analysis of 100 Gb/s demultiplexing using nonlinear optical loop mirror," *J. Lightwave Technol.*, vol. 15, pp. 194–201, Feb. 1997.

[22] J. W. Lou, J. K. Andersen, J. C. Stocker, M. N. Islam, and D. A. Nolan, "Polarization insensitive demultiplexing of 100-Gb/s words using a twisted fiber nonlinear optical loop mirror," *IEEE Photon. Technol. Lett.*, vol. 11, pp. 1602–1604, Dec. 1999.

[23] N. J. Doran and D. Wood, "Nonlinear-optical loop mirror," *Opt. Lett.*, vol. 13, no. 1, pp. 56–58, Jan. 1988.

[24] M. Jinno, "All-optical signal regularizing/regeneration using a nonlinear fiber sagnac interferometer switch with signal-clock walk-off," *J. Lightwave Technol.*, vol. 12, pp. 1648–1659, Sept. 1994.

[25] S. J. Savage, B. S. Robinson, S. A. Hamilton, and E. P. Ippen, "All-optical pulse regeneration in an ultrafast nonlinear interferometer with Faraday mirror polarization control," *Tech. Dig. Conf. Lasers and Electro-Opt.*, vol. 56, 2001.

[26] N. S. Patel, K. L. Hall, and K. A. Rauschenbach, "Interferometric all-optical switches for all-optical signal processing," *Appl. Opt.*, vol. 37, no. 14, pp. 2831–2842, May 1998.

[27] K. L. Hall and K. A. Rauschenbach, "100 Gbit/s bitwise logic," *Opt. Lett.*, vol. 23, no. 16, pp. 1271–1273, Aug. 1998.

[28] A. J. Poustie, K. J. Blow, R. J. Manning, and A. E. Kelly, "All-optical pseudorandom number generator," *Opt. Commun.*, vol. 159, pp. 208–214, Jan. 1999.

[29] B.-E. Olsson and P. A. Andrekson, "Polarization-indpendent all-optical AND-gate using randomly birefringent fiber in a nonlinear optical loop mirror," *Tech. Dig. Opt. Fiber Commun. Conference and Exhibit*, vol. 2, 1998.

[30] B. S. Robinson, S. A. Hamilton, S. J. Savage, and E. P. Ippen, "40 Gbit/s all-optical XOR using a fiber-based folded ultrafast nonlinear interferometer," *Tech. Dig. Opt. Fiber Commun. Conf.*, vol. 70, 2002.

[31] K. Tajima, "All-optical switch with switch-off time unrestricted by carrier lifetime," *Jpn. J. Appl. Phys.*, vol. 32, no. 12A, pp. 1746–1749, Dec. 1993.

[32] D. Wolfson, A. Kloch, T. Fjelde, C. Janz, B. Dagens, and M. Renaud, "40 Gb/s all-optical wavelength conversion, regeneration, and demultiplexing in an SOA-based all-active Mach-Zehnder interferometer," *IEEE Photon. Technol. Lett.*, vol. 12, pp. 332–334, Mar. 2000.

[33] S. Diez, C. Schubert, R. Ludwig, H.-J. Ehrke, U. Feiste, C. Schmidt, and H. G. Weber, "160 Gbit/s all-optical demultiplexer using hybrid gain-transparent SOA Mach-Zehnder interferometer," *Electron. Lett.*, vol. 36, no. 17, pp. 1484–1486, Aug. 2000.

[34] M. Dulk, S. Fischer, M. Bitter, M. Caraccia, W. Vogt, E. Gini, H. Melchior, W. Hunziker, A. Buxens, H. N. Poulsen, and A. T. Clausen, "Ultrafast all-optical demultiplexer based on monolithic Mach-Zehnder interferometer with integrated semiconductor optical amplifiers," *Opt. and Quantum Electron.*, vol. 33, pp. 899–906, 2001.

[35] P. V. Studenkov, M. R. Gokhale, J. Wei, W. Lin, I. Glesk, P. R. Prucnal, and S. R. Forrest, "Monolithic integration of an all-optical Mach-Zehnder demultiplexer using an asymmetric twin-waveguide structure," *IEEE Photon. Technol. Lett.*, vol. 13, pp. 600–602, June 2001.

[36] S. Nakamura, Y. Ueno, and K. Tajima, "Error-free all-optical demultiplexing at 336 Gb/s with a hybrid-integrated symmetric-Mach-Zehnder switch," *Tech. Dig. Optical Fiber Commun. Conf.*, vol. 70, 2002.

[37] L. H. Spiekman, U. Koren, M. D. Chien, B. I. Miller, J. M. Wiesenfeld, and J. S. Perino, "All-optical Mach-Zehnder wavelength converter with monolithically integrated DFB probe source," *IEEE Photon. Technol. Lett.*, vol. 9, pp. 1349–1351, Oct. 1997.

[38] T. Fjelde, D. Wolfson, A. Kloch, C. Janz, A. Coquelin, I. Guillemot, F. Gaborit, F. Poingt, B. Dagens, and M. Renaud, "10 Gbit/s all-optical logic OR in monolithically integrated interferometric wavelength converter," *Electron. Lett.*, vol. 36, pp. 813–815, Apr. 2000.

[39] T. Fjelde, D. Wolfson, A. Kloch, B. Dagens, A. Coquelin, I. Guillemot, F. Gaborit, F. Poingt, and M. Renaud, "Demonstration of 20 Gbit/s all-optical logic XOR in integrated SOA-based interferometric wavelength converter," *Electron. Lett.*, vol. 36, no. 22, pp. 1863–1864, Oct. 2000.

[40] K. L. Hall, G. Lenz, A. M. Darwish, and E. P. Ippen, "Subpicosecond gain and index nonlinearities in InGaAsP diode lasers," *Opt. Commun.*, vol. 111, pp. 589–612, Oct. 1994.

[41] R. J. Manning, D. A. O. Davies, D. Cotter, and J. K. Lucek, "Enhanced recovery rates in semiconductor laser amplifiers using optical pumping," *Electron. Lett.*, vol. 30, no. 10, pp. 787–788, May 1994.

[42] G. E. Shtengel, D. A. Ackerman, and P. A. Morton, "True carrier lifetime measurements of semiconductor lasers," *Electron. Lett.*, vol. 31, no. 20, pp. 1747–1748, Sep. 1995.

[43] H. K. Kim and S. Chandrasekhar, "Reduction of cross-gain modulation in the semiconductor optical amplifier by using wavelength modulated signal," *IEEE Photon. Technol. Lett.*, vol. 12, no. 10, pp. 1412–1414, Oct. 2000.

[44] A. K. Srivastava, S. Banerjee, B. R. Eichenbaum, C. Wolf, Y. Sun, J. W. Sulhoff, and A. R. Chraplyvy, "A polarization multiplexing technique to mitigate WDM crosstalk in SOA's," *IEEE Photon. Technol. Lett.*, vol. 12, pp. 1415–1416, Oct. 2000.

[45] B. S. Robinson, J. D. Moores, and D. T. Moriarty, "Pattern independent semiconductor-based interferometric all-optical switching using pulse position modulation," *Tech. Dig. Conf. Lasers and Electro-Opt.*, vol. 56, 2000.

[46] K. Suzuki, K. Iwatsuki, S. Nishi, M. Saruwatari, and T. Kitoh, "160 Gbit/s sub-picosecond transform-limited pulse signal generation utilizing adiabatic soliton compression and optical time-division multiplexing," *IEEE Photon. Technol. Lett.*, vol. 6, pp. 352–354, Mar. 1994.

[47] T. J. Xia, Y.-H. Kao, Y. Liang, J. W. Lou, K. H. Ahn, O. Boyraz, G. A. Nowak, A. A. Said, and M. N. Islam, "Novel self-synchronization scheme for high-speed packet TDM networks," *IEEE Photon. Technol. Lett.*, vol. 11, pp. 269–271, Feb. 1999.

[48] M. Nakazawa, H. Kubota, K. Suzuki, E. Yamada, and A. Sahara, "Ultrahigh-speed long-distance TDM and WDM soliton transmission technologies," *IEEE J. Select Topics Quantum Electron.*, vol. 6, pp. 363–396, Mar./Apr. 2000.

[49] I. Glesk, J. P. Sokoloff, and P. R. Prucnal, "All-optical address recognition and self-routing in a 250 Gbit/s packet-switched network," *Electron. Lett.*, vol. 30, no. 16, pp. 1322–1323, Aug. 1994.

[50] D. Cotter, J. K. Lucek, M. Shabeer, K. Smith, D. C. Rogers, D. Nesset, and P. Gunning, "Self-routing of 100 Gbit/s packets using 6 bit 'keyword' address recognition," *Electron. Lett.*, vol. 31, no. 25, pp. 2201–2202, Dec. 1995.

[51] T. J. Xia, Y. Liang, K. H. Ahn, J. W. Lou, O. Boyraz, Y.-H. Kao, X. D. Cao, S. Chaikamnerd, J. K. Andersen, and M. N. Islam, "All-optical packet-drop demonstration using 100 Gbit/s words by integrating fiber-based components," *IEEE Photon. Technol. Lett.*, vol. 10, pp. 153–155, Dec. 1998.

[52] S. A. Hamilton, B. S. Robinson, J. D. Moores, F. Hakimi, and P. A. Schulz, "Ultrafast synchronous all-optical time division multiplexing system demonstration," *Tech. Dig. Opt. Fiber Commun. Conf.*, vol. 54, 2001.

[53] S. A. Hamilton and B. S. Robinson, "40 Gbit/s all-optical packet synchronization and address comparison for OTDM networks," *IEEE Photon. Technol. Lett.*, vol. 14, pp. 209–211, Feb. 2002.

[54] ——, "100 Gbit/s synchronous all-optical time-division multiplexing multi-access network testbed," *Tech. Dig. Optical Fiber Commun. Conf.*, vol. 70, 2002.
[55] M. Nakazawa, T. Yamamoto, and K. R. Tamura, "1.28 Tbit/s-70 km OTDM transmission using third- and fourth-order simultaneous dispersion compensation with a phase modulator," *Electron. Lett.*, vol. 36, no. 24, pp. 2027–2029, Nov. 2000.
[56] J. P. Gordon and H. A. Haus, "Random walk of coherently amplified solitons in optical fiber transmission," *Opt. Lett.*, vol. 11, no. 10, pp. 665–667, Oct. 1986.
[57] B. S. Robinson, S. A. Hamilton, and E. P. Ippen, "Demultiplexing of 80 Gbit/s pulse-position modulated data with an ultrafast nonlinear interferometer," *IEEE Photon. Technol. Lett.*, vol. 14, pp. 206–208, Feb. 2002.
[58] D. Marquis, "BoSSNET: An all-optical long haul networking testbed," *Tech. Dig. Lasers and Electro-Opt. Soc. Ann. Meeting*, vol. 1, 2000.
[59] T. Hirooka, T. Nakada, and A. Hasagawa, "Feasibility of densely dispersion managed soliton transmission at 160 Gb/s," *IEEE Photon. Technol. Lett.*, vol. 12, pp. 633–635, June 2000.
[60] J. Martensson and A. Berntson, "Dispersion-managed solitons for 160-Gb/s data transmission," *IEEE Photon. Technol. Lett.*, vol. 13, pp. 666–668, July 2001.
[61] U. Feiste, R. Ludwig, C. Schubert, J. Berger, C. Schmidt, H. G. Weber, B. Schmauss, A. Munk, B. Buchold, D. Briggman, F. Keuppers, and F. Rumpf, "160 Gbit/s transmission over 116 km field-installed fiber using 160 Gbit/s OTDM and 40 Gbit/s ETDM," *Electron. Lett.*, vol. 37, no. 7, pp. 443–445, Jan. 2001.
[62] B. Mikkelsen, G. Raybon, R.-J. Essiambre, A. J. Stentz, T. N. Nielsen, D. W. Peckham, L. Hsu, L. Gruner-Nielson, K. Dreyer, and J. E. Johnson, "320-Gb/s single-channel pseudolinear transmission over 200 km of nonzero-dispersion fiber," *IEEE Photon. Technol. Lett.*, vol. 12, pp. 1400–1402, Oct. 2000.
[63] A. Royset and R. I. Laming, "Demonstration of standard fiber transmission limited by third-order dispersion," *Tech. Dig. Opt. Commun. Conf.*, vol. 2, 1996.
[64] D. Marcuse and C. R. Menyuk, "Simulation of single-channel optical systems at 100 Gb/s," *J. Lightwave Technol.*, vol. 17, pp. 564–569, Apr. 1999.
[65] J. F. Brennan, E. Hernandez, J. A. Valenti, P. G. Sinha, M. R. Matthews, D. E. Elder, G. A. Beauchesne, and C. H. Byrd, "Dispersion and dispersion-slope correction with a fiber Bragg grating over the full C-band," *Tech. Dig. Opt. Fiber Commun. Conf.*, vol. 54, 2001.
[66] C. S. Goh, S. Y. Set, K. Taira, S. K. Khijwania, and K. Kikuchi, "Nonlinearly strain-chirped fiber Bragg grating with an adjustable dispersion slope," *IEEE Photon. Technol. Lett.*, vol. 14, pp. 663–665, May 2002.
[67] S. Watanabe and M. Shirasaki, "Exact compensation for both chromatic dispersion and Kerr effect in a transmission fiber using phase conjugation," *J. Lightwave Technol.*, vol. 14, pp. 243–248, Mar. 1996.
[68] T. Yamamoto and M. Nakazawa, "Third- and fourth-order active dispersion compensation with a phase modulator in a terabit-per-second optical time-division multiplexed transmission," *Opt. Lett*, vol. 26, no. 9, pp. 647–649, May 2001.
[69] T. Yamamoto, E. Yoshida, K. R. Tamura, K. Yonenaga, and M. Nakazawa, "640 Gbit/s optical TDM transmission over 92 km through a dispersion-managed fiber consisting of single-mode fiber and reverse dispersion fiber," *IEEE Photon. Technol. Lett*, vol. 12, pp. 353–355, Mar. 2000.
[70] A. R. Chraplyvy, "Limitations on lightwave communications imposed by optical-fiber nonlinearities," *J. Lightwave Technol.*, vol. 8, pp. 1548–1557, Oct. 1990.
[71] N. Shibata, K. Nosu, K. Iwashita, and Y. Azuma, "Transmission limitations due to fiber nonlinearities in optical FDM systems," *IEEE J. Select. Areas Commun.*, vol. 8, pp. 1068–1077, Aug. 1990.
[72] R. W. Tkach, A. R. Chraplyvy, F. Forghieri, A. H. Gnauck, and R. M. Derosier, "Four-photon mixing and high-speed WDM systems," *J. Lightwave Technol.*, vol. 13, pp. 841–849, May 1995.
[73] N. Takachio and S. Ohteru, "Scale of WDM transport network using different types of fibers," *IEEE J. Select. Areas Commun.*, vol. 16, pp. 1320–1326, Sept. 1998.
[74] T. Yu, E. A. Golovchenko, A. N. Pilipetskii, and C. R. Menyuk, "Dispersion-managed soliton interactions in optical fibers," *Opt. Lett.*, vol. 22, no. 11, pp. 793–795, June 1997.
[75] P. V. Mamyshev and N. A. Mamysheva, "Pulse-overlapped dispersion-managed data transmission and intrachannel four-wave mixing," *Opt. Lett.*, vol. 24, no. 21, pp. 1454–1456, Nov. 1999.
[76] R.-J. Essiambre, B. Mikkelsen, and G. Raybon, "Intra-channel cross-phase modulation and four-wave mixing in high-speed TDM systems," *Electron. Lett.*, vol. 35, no. 18, pp. 1576–1578, Sept. 1999.
[77] L. Möller, Y. Su, G. Raybon, S. Chandrasekhar, and L. L. Buhl, "Penalty interference of nonlinear intra-channel effects and PMD in ultra high-speed TDM systems," *Electron. Lett.*, vol. 38, no. 6, pp. 281–283, Mar. 2002.
[78] T. Hirooka and M. J. Ablowitz, "Analysis of timing jitter and amplitude jitter due to intrachannel dispersion-managed pulse interactions," *IEEE Photon. Technol. Lett.*, vol. 14, pp. 633–635, May 2002.
[79] S. Kumar, J. C. Mauro, S. Raghavan, and D. Q. Chowdhury, "Intrachannel nonlinear penalties in dispersion-managed transmission systems," *IEEE J. Select. Topics Quantum Electron.*, vol. 8, pp. 626–631, May/June 2002.
[80] M. Jinno and T. Matsumoto, "Optical tank circuits for all-optical timing recovery," *IEEE J. Quantum. Electron*, vol. 28, pp. 895–900, Apr. 1992.
[81] K. Smith and J. K. Lucek, "All-optical clock recovery using a mode-locked laser," *Electron. Lett.*, vol. 28, no. 19, pp. 1814–1816, Sept. 1992.
[82] A. D. Ellis, T. Widdowson, X. Shan, G. E. Wickens, and D. M. Spirit, "Transmission of a true single polarization 40 Gbit/s soliton data signal over 205 km using a stabilized erbium doped fiber ring laser and 40 GHz electronic timing recovery," *Electron. Lett.*, vol. 29, no. 11, pp. 990–992, May 1993.
[83] T. F. Carruthers and J. W. Lou, "80 to 10 Gbit/s clock recovery using phase detection with Mach-Zehnder modulator," *Electron. Lett.*, vol. 37, no. 14, pp. 906–907, July 2001.
[84] O. Kamatani and S. Kawanishi, "Ultrahigh-speed clock recovery with phase lock loop based on four-wave mixing in a traveling-wave laser diode amplifier," *J. Lightwave Technol.*, vol. 14, pp. 1757–1767, Aug. 1996.
[85] S. Fischer, M. Dulk, E. Gamper, W. Vogt, E. Gini, H. Melchior, W. Hunziker, D. Nesset, and A. D. Ellis, "Optical 3R regenerator for 40 Gbit/s networks," *Electron. Lett.*, vol. 35, no. 23, pp. 2047–2049, Nov. 1999.
[86] J. Leuthold, B. Mikkelsen, R. E. Behringer, G. Raybon, C. H. Joyner, and P. A. Besse, "Novel 3R regenerator based on semiconductor optical amplifier delayed-interference configuration," *IEEE Photon. Technol. Lett.*, vol. 13, pp. 860–862, Aug. 2001.
[87] K. S. Jepsen, A. Buxens, A. T. Clausen, H. N. Poulsen, B. Mikkelsen, and K. E. Stubkjaer, "20 Gbit/s optical 3R regeneration using polarization-independent monolithically integrated Michelson interferometer," *Electron. Lett.*, vol. 34, no. 5, pp. 472–474, Mar. 1998.
[88] T. Otani, T. Miyazaki, and S. Yamamoto, "40-Gb/s optical 3R regenerator using electroabsorption modulators for optical networks," *J. Lightwave Technol.*, vol. 20, pp. 195–200, Feb. 2002.
[89] C. Vinegoni, M. Wegmuller, B. Huttner, and N. Gisin, "All optical switching in a highly birefringent and a standard telecom fiber using a Faraday mirror stabilization scheme," *Opt. Commun.*, vol. 182, pp. 335–341, Aug. 2000.
[90] I. Shake, H. Takara, K. Uchiyama, S. Kawanishi, and Y. Yamabayashi, "Vibration-insensitive nonlinear optical loop mirror utilizing reflective scheme," *IEEE Photon. Technol. Lett.*, vol. 12, pp. 555–557, May 2000.

Scott A. Hamilton (S'90–M'99) was born in Ridgecrest, CA, on March 10, 1970. He studied electrical engineering and received the B.S. degree (with high honors) from the University of California, Davis, in 1993, and the M.S. and Ph.D. degrees in electrical engineering in 1996 and 1999.

In 1993, he joined the Microphotonics Laboratory at UC Davis where he pursued research in optical modulators for analog RF-photonics applications. From 1989 to 1998, he worked for the Aircraft Systems Engineering Branch at the Naval Air Warfare Center, China Lake, CA. In 2000, he joined the Optical Communications Technology Group at MIT Lincoln Laboratory where he is conducting research on optical time-division multiaccess networks. His research interests include high-speed short-pulse communication systems, optical packet switching, ultrafast optical signal processing, nonlinear optics, and integrated microphotonics.

Dr. Hamilton is a member of the Optical Society of America, IEEE/LEOS, Tau Beta Pi, Pi Mu Epsilon, Phi Kappa Phi, and the Golden Key Honor Society.

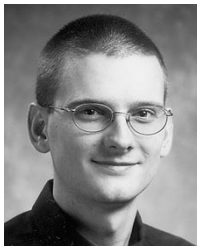

Bryan S. Robinson (S'02) was born in Dallas, TX, in November 1975. In 1998, he received the S.B. degrees in mathematics and electrical engineering and the M.Eng. degree in electrical engineering from the Massachusetts Institute of Technology (MIT). He is currently pursuing the Ph.D. degree in electrical engineering at MIT.

Since 1996, he has been working with the Optical Communications Technology group and Advanced Networks group at MIT Lincoln Laboratory. His research interests include ultrafast time-division multiplexed networks, semiconductor- and fiber-based all-optical switching, gain-saturation in semiconductors, and numerical modeling of semiconductor optical amplifiers.

In 1998, Mr. Robinson was awarded a National Science Foundation research fellowship. In 2001, he received the LEOS Research Fellowship. He is a member of Eta Kappa Nu and Tau Beta Pi.

Thomas E. Murphy (M'98) was born in Falls Church, VA. He studied physics and electrical engineering at Rice University, graduating with joint B.A./B.S.E.E. degrees (*summa cum laude*) in 1994. He received the M.S. degree in 1997 and the Ph.D. degree in 2000 from Massachusetts Institute of Technology (MIT), Cambridge.

In 1994, he joined the NanoStructures Laboratory at MIT, where he pursued research in integrated optics and nanotechnology. He was awarded a National Science Foundation fellowship in 1994 for graduate research, and in 2000 he and his colleagues received the Lemelson-MIT student team prize for innovation in telecommunications and networking. In 2000, he joined MIT Lincoln Laboratory as a staff member in the Optical Communications Technology Group where he studied and developed ultrafast optical communications systems. In August 2002, he joined the faculty at the University of Maryland, College Park, as an Assistant Professor in the Department of Electrical and Computer Engineering. His research interests include optical communications, short-pulse phenomena, numerical simulation, optical pulse propagation, nanotechnology, and integrated photonics.

Professor Murphy is a member of the Optical Society of America, Tau Beta Pi, and Sigma Xi.

Shelby Jay Savage (S'98–M'00) was born in Robins AFB, GA, on May 25, 1978. He received the S.B. degree in mathematics in 2000 and the S.B. and M.Eng. degrees in electrical engineering in 2001 from the Massachusetts Institute of Technology (MIT), Cambridge, and is currently pursuing the Ph.D. degree in electrical engineering at MIT.

Since 1998, he has worked with the Optical Communications Technology group and Advanced Networks group of MIT Lincoln Laboratory. His research interests include all-optical switching, all-optical regeneration, and short optical pulse generation.

Mr. Savage is a member of Eta Kappa Nu and Tau Beta Pi.

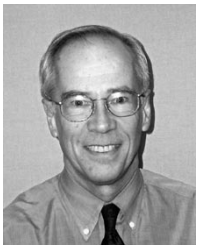

Erich P. Ippen (S'66–M'69–SM'81–F'84) received the S.B. degree in electrical engineering from the Massachusetts Institute of Technology (MIT), Cambridge, in 1962 and the M.S. and Ph.D. degrees in the same field from the University of California in 1965 and 1968, respectively.

He was Member of Technical Staff at Bell Laboratories, Holmdel, NJ, from 1968 to 1980. In 1980, he joined the faculty of MIT, where he is now Elihu Thomson Professor of Electrical Engineering and Professor of Physics. His research interests have included nonlinear optics in fibers, femtosecond pulse generation, ultrafast processes in materials and devices, photonic-bandgap structures, and ultrashort-pulse fiber devices.

Professor Ippen is a Fellow of the American Physical Society and the Optical Society of America. He is a member of the National Academy of Sciences, the National Academy of Engineering, and the American Academy of Arts and Sciences.